Morphology-dependent energy transfer within polyfluorene thin films

Amena L. T. Khan, Paiboon Sreearunothai, Laura M. Herz, Michael J. Banach, and Anna Köhler*
Cavendish Laboratory, University of Cambridge, Madingley Road, Cambridge CB3 0HE, United Kingdom
(Received 23 June 2003; published 4 February 2004)

We have performed a detailed study of the photoluminescence from thin films of blue-light-emitting poly(9,9-dioctylfluorene) containing different fractions of planarized (β-phase) chains within the glassy polymer film. By choosing solvents with a range of polarities and boiling points we were able to cast films with reliable control of the relative amounts of β-phase chains present. We analyzed the emission spectra in terms of Franck-Condon progressions and found that, at low temperatures (8 K), the luminescence can be modeled accurately by considering two distinct contributions from the two phases present in the film. The Huang-Rhys parameter for the β phase is shown to be approximately half the value obtained for the glassy phase, in agreement with a more delocalized exciton in the β phase. Time-resolved photoluminescence measurements on a film containing roughly 25% of β phase reveal a fast transfer of excitations from the glassy to the β phase, indicating that the two phases are well intermixed. Assuming the transfer dynamics to be governed by dipole-dipole coupling, we obtain a Förster radius of 8.2 ± 0.6 nm, significantly larger than the radius typically found for excitation transfer within the glassy phase. These results are consistent with the large spectral overlap between the emission of the glassy phase and the absorption of the β phase and explain why the latter dominates the emission even from films containing only a small fraction of β-phase chains.

DOI: 10.1103/PhysRevB.69.085201 PACS number(s): 78.47.+p, 33.20.Tp, 78.55.Kz, 78.66.Qn

I. INTRODUCTION

Polyfluorenes are a class of organic semiconductors that have been intensely researched over the past few years,[1,2] as they combine efficient blue luminescence with the possibility of chain alignment, allowing light-emitting diodes to be made with linearly polarized emission.[3–5] The photophysical properties of polyfluorenes are known to vary strongly with the morphology of the film.[1,2] In poly(9,9-dioctylfluorene) (PFO), distinct phases have been identified, such as the disordered glassy phase obtained by spin coating from a good solution, and crystalline α and β phases where the PFO chains are considered to be planar, with a longer intrachain correlation and conjugation length in the β phase than in the α phase.[6]

The fraction of planarized chains was found to determine the number of triplet excitons and polarons formed in a film[7,8] and the photoluminescence efficiency.[9] Having good control over the formation of these phases is therefore crucial for the performance of light-emitting diodes. Previous attempts to control the morphology of PFO thin films include thermal and vapor treatment of as-cast films, although morphological differences have also been observed by simply casting films from a variety of solvents.[1,2,6,10,11]

The presence of β-phase chains can be identified in absorption measurements by a peak at about 436 nm, just below the main absorption band, and in emission measurements by a vibronic structure that closely resembles the emission of ladder-type poly-*para*-phenylene (LPPP), where the poly(*p*-phenylene) backbone has a fully planarized chemical structure. As glassy and crystalline phases can coexist in a polymer film, their emission spectra are sometimes superimposed and can be difficult to separate unless one phase dominates. Nevertheless, Ariu and co-workers note a strong fraction of luminescence from planarized chains in the emission spectra, even when their contribution to the absorption is low, and suggest that energy migration onto β-phase chains might occur.[9,12] We performed a detailed study of energy transfer from the glassy to the β phase using time-resolved spectroscopy and deduce a large Förster radius of about 8.2 nm. Good control over the formation of the β phase was obtained by spinning thin films from solvents with different polarities and boiling points. We perform a Franck-Condon analysis of the luminescence to obtain the Huang-Rhys parameters of the glassy and β phases along with the relative contributions of either phase to the overall emission.

II. EXPERIMENTAL METHOD

All measurements were made using thin films with a typical thickness of 50–100 nm spun onto quartz substrates from chloroform, toluene, xylene, isodurene, and cyclopentanone solutions of the polymer using a conventional photoresist spin coater. For temperature-dependent absorption measurements, the samples were held in a temperature-controlled continuous flow helium cryostat. Illumination was provided by a 150 W xenon arc lamp dispersed by a Jobin-Yvon monochromator. The transmission was measured with a UV-enhanced silicon photodiode and a Stanford Research lock-in amplifier (SR830). The spectra were corrected for the transmission of the setup. The optical absorption spectra at room temperature were also compared to those measured with a Hewlett-Packard ultraviolet-visible spectrometer and found to be identical. Raman spectra were taken with a Renishaw Raman microscope connected to a spectrometer with a charge-coupled device (CCD) camera. The excitation wavelength was the 632.8 nm line of a HeNe laser.

Measurements of photoluminescence (PL) were made with the sample in a continuous-flow helium cryostat. Excitation was provided by the UV lines (355 and 365 nm) of a continuous wave (cw) argon ion laser. Typical intensities used were a few mW/mm^2. The emission spectra were re-

 ©2004 The American Physical Society

corded using a spectrograph with an optical fiber input coupled to a cooled CCD array (Oriel Instaspect IV). Time-resolved photoluminescence spectroscopy was performed at room temperature using the up-conversion technique. The sample was excited with the frequency-doubled output from a mode-locked Ti:sapphire laser supplying 200 fs pulses at an energy of 3.06 eV and a repetition rate of 76 MHz. The average excitation power was 0.6 mW on a spot of about 110 μm diameter. Photoluminescence originating from the sample was collected using dispersion-free optics and up-converted in a β barium borate crystal using the fundamental laser beam at 1.53 eV as a gate. Sum-frequency photons were dispersed in a monochromator, and detected via single-photon counting. To set the detection polarization with respect to the excitation polarization, the latter was adjusted by rotation of a $\lambda/2$ plate and a Glan-Thompson polarizing prism. All up-conversion measurements shown were taken for collinearly polarized exciting and detected light. The overall temporal resolution was 380 fs, while the spectral resolution of the system was approximately 20 meV. All time-resolved PL spectra were corrected for spectral response by up-converting the light originating from a W filament lamp with known emissivity. The sample was held at a pressure of less than 10^{-6} mbar during measurements to avoid photo-oxidation.

III. RESULTS AND DISCUSSION

A. Absorption and photoluminescence spectroscopy

Figure 1 shows the absorption and emission spectra at room temperature from thin films spun from chloroform, toluene, xylene, isodurene, and cyclopentanone solutions. The characteristics of the various solvents are summarized in Table I. We observe the 0-0 and 0-1 vibrational peaks of the absorption due to the crystalline β phase at 2.84 and about 3.08 eV, respectively,[10,13] for the films spun from cyclopentanone, isodurene, and, to a lesser extent, xylene solution. The absorption of films spun from chloroform or toluene solution shows no such features and is shifted further to the blue. We use the intensity of the 0-0 β-phase peak to scale the β-phase absorption spectrum[1] and thus to estimate the fraction of the total absorption originating from the planarized chains (Table I).

An increased formation of planar chains upon spin coating has previously been attributed to poor solvent quality.[10] The character of a solvent can be parametrized in terms of the solubility parameter δ (also referred to as the Hildebrand parameter), which gives a measure for the attractive strength between molecules of a material and corresponds to the square root of the cohesive energy density.[14] The enthalpy of mixing, ΔH, between polymer and solvent depends on the difference in the solubility parameters of polymer and solvent $[\Delta H/V=(\delta_{\text{polymer}}-\delta_{\text{solvent}})^2\ \Phi_{\text{polymer}}\Phi_{\text{solvent}}$, where V is the volume of the mixture and Φ is the volume fraction], so good mixing is observed when polymer and solvent have the same δ. On this basis, Grell and co-workers have inferred a δ of about 9.1–9.3 $(\text{cal/cm}^3)^{1/2}$ for PFO.[10] However, Fig. 1(a) suggests that, in addition to the solubility parameter, the boiling point of the solvent may also play a vital role in determining the β-phase concentration of a spun-cast film. For example, isodurene and chloroform have the same δ, yet only the film spun from isodurene has a significant fraction of β phase. Similarly, toluene and xylene have very close solubility parameters yet give rise to different amounts of β phase. In either case the solvent with the higher boiling point has an increased β-phase concentration. This fact might help explain the mechanism that promotes β-phase formation in spun-cast films. β-phase formation was also observed after slow thermal cycling or exposure to solvent vapor. It was argued that the thermal contraction and expansion cycles or the swelling induced by solvent vapor may cause a mechanical stress which causes the polyfluorene chains to adopt a planar conformation.[6,15] We consider that a similar mechanical stress may apply during spin casting from a moderately poor solvent. A poor solvation environment may assist a tendency to crystallization. Moreover, the polymer will fall out of solution before the solvent fully dissipates. This mechanism is sensitive not only to thermodynamical parameters like the enthalpy of mixing, but also to the kinetics of film formation, and it can therefore be influenced by the boiling point of the solvent. When the boiling point is low, as for chloroform, there is little time between the polymer falling out of solution and the film drying. In contrast, in a solvent with high boiling point such as isodurene, the solution be-

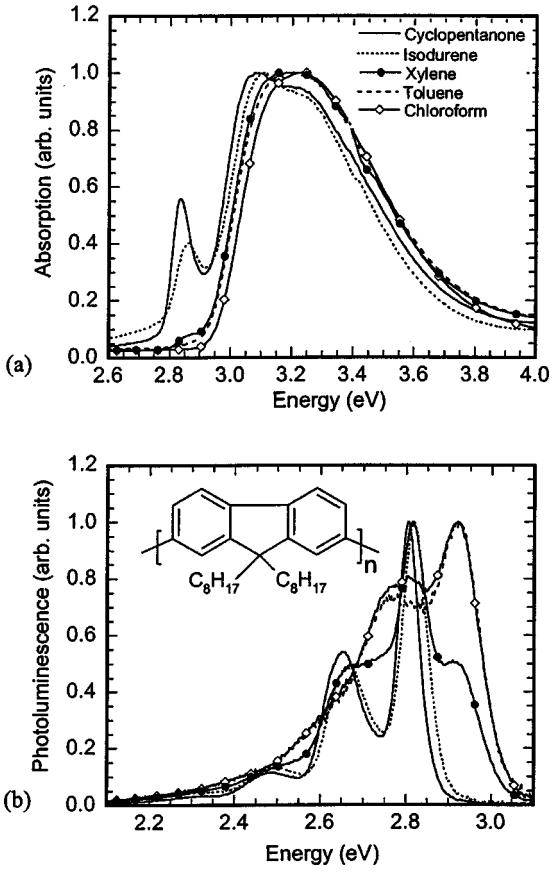

FIG. 1. Room temperature absorption (a) and luminescence (b) spectra of thin films of PFO spun from various solvents as indicated in the figure. The inset shows the chemical structure of PFO.

TABLE I. Fraction of β phase for the different solvents together with their boiling points and polarities.

Solvent	β-phase fraction absorption (300 K)	β-phase fraction emission (10 K)	Boiling point (°C)	Solubility parameter δ_p $(\text{cal/cm}^3)^{1/2}$
Chloroform	<0.01	0.10	61	9.3
Toluene	<0.01		110	8.9
Xylene	0.01–0.05	0.44	138	8.8
Isodurene	0.20	1.00	198	9.3
Cyclopentanone	0.25	1.00	130	10.4

comes increasingly concentrated during spin casting, until eventually the polymer falls out while the film is still wet and spinning. It can thus be stressed by the remaining escaping solvent. We note that we found the fraction of β-phase formation by spin coating to be well reproducible, except for xylene where some variation occurred.

Figure 1(b) shows that the fraction of emission originating from the β phase varies more strongly with solvent than the fraction of absorption observed in Fig. 1(a). In the cyclopentanone- and isodurene-spun films, the planarized chains account for 20% and 25% of the total absorption. However, all of the emission from these films appears to come from the β phase; the 0-0 peak of the emission is at about 2.81 eV, and the vibronic structure is characteristic for β-phase emission.[1] This suggests an efficient mechanism of energy transfer from nonplanar, disordered chains in the glassy phase to planar chains in the crystalline phase. In contrast, in the films spun from chloroform and toluene, we observe emission mainly from the nonplanar, disordered chains; the 0-0 peak of emission occurs at 2.91 eV and the vibronic structure is different. The film spun from xylene seems to be a superposition of the two extreme cases.

From here onward we will consider only the solvents cyclopentanone, xylene, and chloroform as a representative of each case. In order to determine accurately the fraction of emission from the glassy and β phases we have performed a Franck-Condon analysis on the low-temperature spectra shown in Fig. 2, which have a higher vibrational resolution than the room temperature spectra. The corresponding absorption spectra are also shown. Overall, the absorption gains vibrational resolution and shifts slightly to the red upon cooling. The low-temperature emission spectrum of the cyclopentanone-spun film very closely resembles that of a fully planar methyl-substituted ladder-type poly-*para*-phenylene (MeLPPP) and has been attributed to β-phase emission.[1] The narrow 0-0 peak of the β-phase emission at 2.78 eV in the cyclopentanone-spun film can be clearly identified as a peak in the xylene-spun film and as a small shoulder in the chloroform-spun film. Thus, some fraction of β-phase emission seems to occur even from the chloroform-spun films. We note that upon cooling the 0-0 position for the luminescence shifts to the red by about 27 meV for both emission from the nonplanar chains in the glassy phase and emission from the planarized chains in the β phase. In fact, a redshift of approximately 20 meV has also been observed for the rigid, fully planar MeLPPP.[16] This confirms the argument put forward by Bässler and Schweitzer which attributes the bathochromic shift to the temperature dependence of the electronic relaxation process rather than the freezing out of torsional modes.[17]

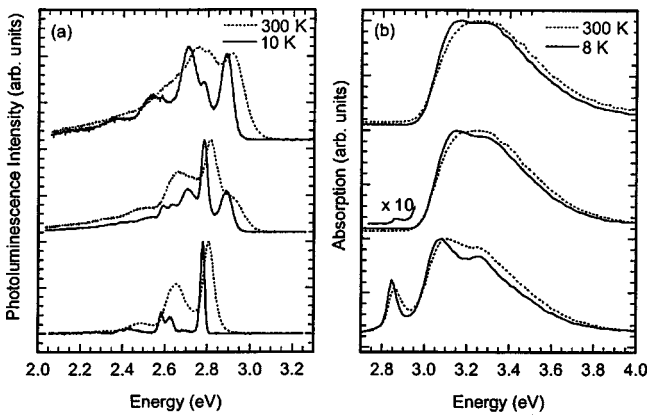

FIG. 2. The luminescence (a) and absorption (b) spectra at 10 and 8 K, respectively, of thin films of PFO spun from chloroform (top), xylene (middle), and cyclopentanone (bottom). The room temperature spectra are also shown for comparison.

A Franck-Condon analysis was carried out on the spectra taken at 10 K. The optical densities at the peak of absorption are 1.55, 0.885, and 1.33 for the films spun from chloroform, xylene, and cyclopentanone, respectively. As evident from Fig. 2, there is no noticeable overlap of absorption and emission for the films spun from chloroform and xylene, and consequently no corrections were made for self-absorption. For the film spun from cyclopentanone, there is a rise in baseline of Fig. 2(b) in the relevant energy range of 2.75–2.80 eV, which can be caused by absorption or increased scattering. Self-absorption would affect the height of the 0-0 peak, and thus the value of the Huang-Rhys parameter. Since there is excellent agreement between the Franck-Condon simulated spectrum and the experimentally measured spectrum even for the 0-2 vibrational transitions (*vide infra*), we consider that self-absorption does not play a significant role, and that the rise in the baseline in Fig. 2(b) reflects an increase in light scattering (which is enhanced in this sample since it contains more microcrystalline domains).

B. Franck-Condon analysis

The vibronic structure of the photoluminescence in conjugated polymers is determined by the Franck-Condon factors. The emission spectrum $P(\hbar\omega)$ in photons/energy interval can be modeled as[18,19]

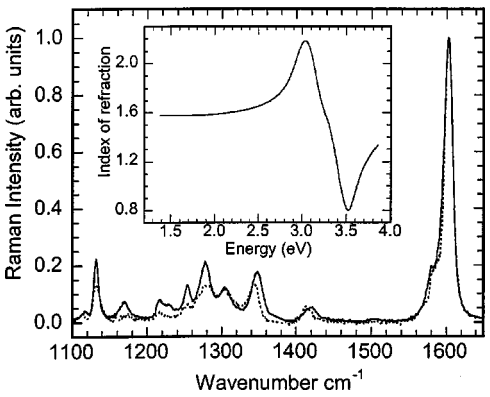

FIG. 3. The Raman spectra of PFO spun from cyclopentanone (solid line) and chloroform (dotted line). The inset shows the refractive index.

$$P(\hbar\omega) = n^3(\hbar\omega)^3 \sum_{n_i=0} I_{0\text{-}n_i} \Gamma\, \delta[\hbar\omega - (\hbar\omega_0 - n_i\hbar\omega_i)], \tag{1}$$

where $\hbar\omega_0$ is the energy of the 0-0 peak, $\hbar\omega_i$ are the vibrational energies of the modes i, $n_i = 0,1,2,3,4$ denotes the number of vibrational overtones, Γ is the Gaussian line shape operator (and was kept at constant full width at half maximum for all modes i and overtones n_i), n is the refractive index, and $I_{0\text{-}n_i}$ is the intensity of the $0\text{-}n_i$ vibronic transition of the mode i. $I_{0\text{-}n_i}$ is related to the Huang-Rhys parameter S_i by[17]

$$I_{0\text{-}n_i} = \frac{e^{-S_i} S_i^{n_i}}{n_i!}. \tag{2}$$

Thus, the ratio of the 0-0 peak to the 0-1 peak gives the Huang-Rhys parameter of a particular vibrational mode.[17] The total Huang-Rhys parameter is the sum over all the individual modes. It is a measure of the difference between the ground and excited state geometries and is related to the relaxation energy E_{rel} by $E_{\text{rel}} = \Sigma_i S_i \hbar\omega_i$.

To determine the vibrational energies $\hbar\omega_i$ we took Raman spectra from the films spun from the three solvents (Fig. 3). The spectrum obtained from xylene is nearly identical to that from chloroform and is therefore not shown. The spectra are characterized by a strong mode at 1605 cm^{-1}, attributed to a ring stretching mode, and a number of modes between 1100 and 1400 cm^{-1} which have been attributed to C-C stretching modes between phenylene rings and C-H in-plane bending modes.[11,12] The peaks in the 1100–1400 cm^{-1} range take a higher relative intensity in the film spun from cyclopentanone, which is rich in β phase, than in the films spun from chloroform or xylene. This is consistent with the higher intensity reported for these peaks by Ariu *et al.* for the vapor-treated film compared to the spin-coated film, where the former has more β phase than the latter.[20] For the Franck-Condon modeling, we considered seven modes i and $n_i = 4$ overtones for each mode. Specifically, we considered mode 7 at 1605 cm^{-1}, modes 6–4, which we placed at about 1137, 1282, and 1411 cm^{-1} to account for the number of peaks in the 1400–1100 cm^{-1} range, and three other lower-energy modes (3–1) taken at 604, 806, and 838 cm^{-1}. The index of refraction was measured by ellipsometry[21] and is shown as the inset to Fig. 3. Its dependence on the photon energy cannot be neglected as is evident from the strong dispersion we observe in the energy range of emission (above 2.6 eV).

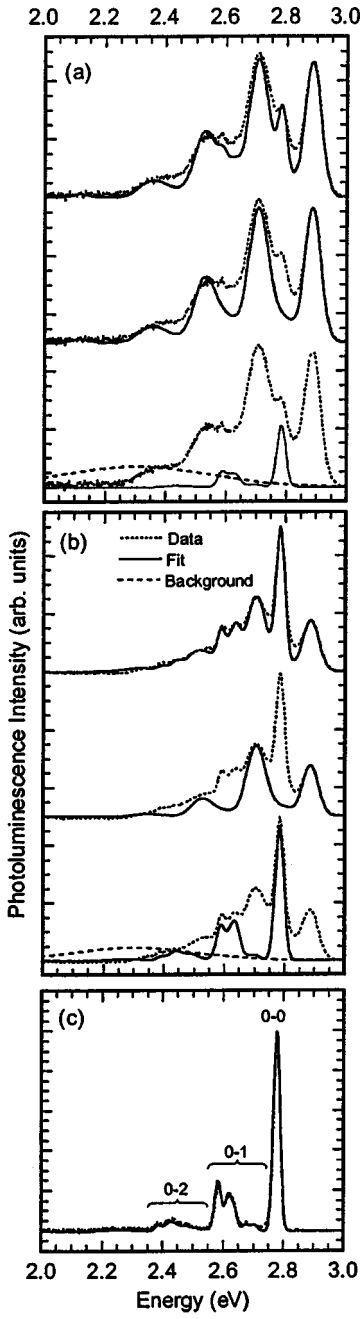

FIG. 4. The photoluminescence spectrum at 10 K of PFO (dotted line) and its Franck-Condon fit (solid line) for a film spun from chloroform (a), xylene (b), and cyclopentanone (c). (a) and (b) show the fits to the β phase, glassy phase, and their sum (offset from bottom to top). A broad Gaussian background was subtracted from the data in (a) and (b) and is also shown (dashed line). In (c), the positions of the 0-0, 0-1, and 0-2 vibrational transitions are indicated for the β phase.

Figure 4 shows the emission together with best fits to Eq.

TABLE II. Huang-Rhys parameters for different phases as extracted from the Franck-Condon analysis of the PL spectra according to the description in the text.

Phase	Linewidth (meV)	E_{rel} (meV)	$\Sigma_i S_i$	S_7	S_{6+5+4}	S_{3+2+1}
β phase in cyclopentanone	25	97	0.58	0.24	0.28	0.06
β phase in xylene or chloroform	34	97	0.58	0.24	0.28	0.06
Glassy phase in chloroform	62	230	1.37	0.46	0.73	0.18
Glassy phase in xylene	64	320	1.87	0.69	0.97	0.21

(1) from the films. To fit the emission, we varied the intensities of the 0-1 transitions for the seven modes, and the Gaussian linewidth, and compared the resulting emission spectrum according to Eq. (1) with the experimental spectrum. Table II lists the total Huang-Rhys parameters and their distribution over the different modes as well as the linewidths and the relaxation energies obtained for the different films. We have grouped the modes $6+5+4$ and $3+2+1$ together as they are energetically closely spaced and the distribution of intensity between them can therefore be varied to some extent without affecting their sum. For the film spun from cyclopentanone, an excellent agreement can be obtained by assuming a single emission with the 0-0 origin at 2.78 eV. We find the β phase to have a low overall Huang-Rhys parameter of 0.6 and a narrow linewidth of 25 meV. The low Huang-Rhys parameter implies not only a well-delocalized excited state, but also that there is little geometric relaxation following a transition from the excited state to the ground state indicating that both states are associated with fairly planar conformations.

In contrast, we were unable to model the emission of the film spun from xylene and chloroform by a single Franck-Condon progression, while a suitable fit was obtained using a superposition of two progressions. To obtain a good fit it was necessary to subtract a broad Gaussian peak centered around 2.3 eV, which we attribute to some aggregation or defect sites.[1] Figures 4(a) and 4(b) show the emission from films spun from chloroform and xylene along with the fit and its two components. We assume one component to be the β phase, taking the 0-0 peak to be at 2.78 eV and using the same Huang-Rhys parameters as determined for the film spun from cyclopentanone solution. A slightly wider Gaussian linewidth of 34 meV is required for a good fit. In the second component we place the 0-0 position at 2.89 eV, the peak position of the glassy phase. We find that this glassy phase has a much wider linewidth of about 62 meV for the chloroform-spun film and 64 meV for the xylene-spun film. The wide linewidth and the associated high amount of inhomogeneous broadening in the glassy phase compared to the crystalline β phase is indicative of a high degree of configurational disorder.[17] The total Huang-Rhys parameter for the glassy phase is 1.4 (1.9) for the chloroform-spun (xylene-spun) film. This is two (three) times the value for the crystalline phase and suggests that significant geometric relaxation occurs after the transition, most likely caused by the transition from a more planar excited state to a nonplanar ground state. Correspondingly, we find the geometric relaxation energy is also two (three) times higher in the glassy phase than in the β phase in the xylene-spun (chloroform-spun) film. We note that the transition from a more planar excited state to a nonplanar ground state is expected to couple to modes associated with torsions between phenyl rings.[22–24] These torsional modes occur around 70 cm^{-1} (about 9 meV), and can therefore not be resolved from the actual 0-0 transition,[22,24,25] yet they cause the Huang-Rhys parameter to be actually underestimated.[22] The values we determine for the Huang-Rhys parameter are in good agreement with the $S=0.65$ estimated by Guha *et al.* for methyl-substituted ladder-type poly-*para*-phenylene and $S=1.2$ for *para*-hexaphenyl.[16] We note that two closely spaced electronic states which depend on the degree of morphological disorder were previously also observed for poly(*para*-phenylene vinylene).[19]

From the fits we have also determined the contribution of either phase to the total emission spectrum given in Table I. In particular, the films spun from xylene and chloroform demonstrate how the emission is sensitively affected even by a small fraction of β phase that is hardly noticeable in the absorption spectrum.

C. Time-resolved photoluminescence from cyclopentanone film

The dominance of β-phase emission from films which contain a relatively small fraction of β-phase chains suggests the existence of a fast transfer of photoexcitations from glassy phase to β-phase chains. This should be expected since the relatively strong overlap between the emission of the glassy phase and the β-phase absorption will allow efficient Förster energy transfer to occur between the two phases, if they are sufficiently well intermixed. In a recent report by Ariu and co-workers, energy transfer was suggested to occur on time scales faster than 5 ps, the time resolution of their system.[12] In order to study the dynamics of this excitation transfer we have here performed time-resolved photoluminescence measurements at room temperature on thin films spun cast from cyclopentanone solution. As mentioned earlier, these films feature a β-phase contribution of 25% to the total absorption both at room temperature and at 8 K (see Fig. 2), while the time-integrated emission is completely dominated by the β phase. These films are therefore ideal samples for investigating the excitation transfer dynamics between the two phases.

Figure 5(a) shows the time-resolved emission spectra of such a film for various times after excitation. At the photon energy of 3.06 eV excitations will be created in both the glassy phase and the β phase, and the emission at early times

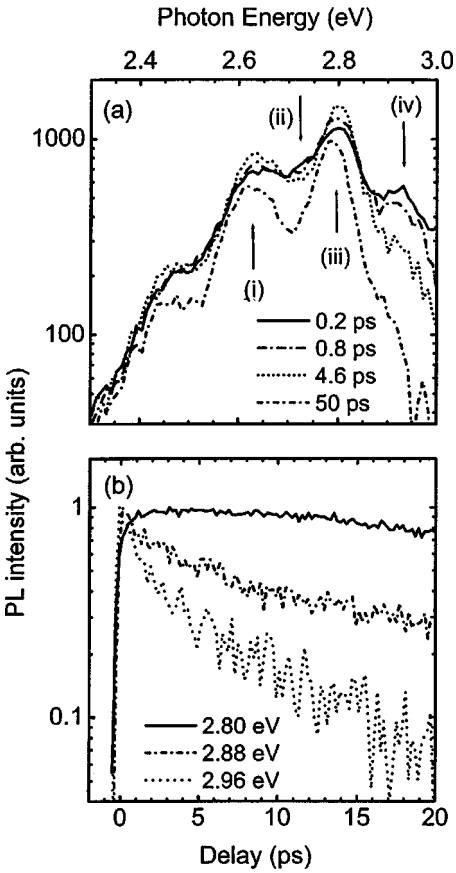

FIG. 5. Time-resolved photoluminescence at room temperature for a PFO film spun from cyclopentanone solution. (a) Spectra for various times after excitation—the arrows indicate the dynamic trends within the first 5 ps after excitation at the different spectral positions. (b) Normalized photoluminescence transients for a range of photon energies.

after excitation should therefore contain both components. This is indeed what we observe: at early times (0.2 ps) the emission spectrum reveals a peak at ≈2.92 eV which we attribute to the (0-0) transition of the glassy phase, while the spectrally narrow peak at 2.80 eV can be identified as the (0-0) emission peak of the β phase. At energies below 2.92 eV the early spectrum is a superposition of both glassy phase and β-phase contributions and the dynamics in the first few picoseconds vary strongly across the spectrum. At 2.93 and 2.72 eV [arrows (ii) and (iv) in Fig. 5(a)] the PL emitted decreases rapidly within the first few picoseconds, while an increase is found at 2.62 and 2.80 eV [arrows (i) and (iii) in Fig. 5(a)]. These changes are further illustrated by the photoluminescence transients given in Fig. 5(b): at 2.96 eV the PL decays rapidly with a 1/*e* time of 3 ps, while an increase on a similar time scale can be seen at 2.80 eV.

The dynamics presented in Fig. 5 strongly suggest that excitation transfer occurs from the glassy phase to the β phase, most of which is completed within a few picoseconds. In order to study the transfer processes in this system in more detail, we focus in the following on the PL decay at 2.96 eV, since the emission in this region of the spectrum is originating solely from the glassy phase. Assuming a transfer mechanism based on Förster dipole-dipole coupling, the emission I_G of the donor (i.e., the glassy phase) can be described by[26,27]

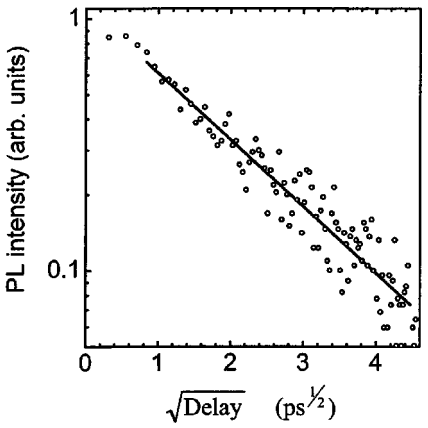

FIG. 6. Photoluminescence at a photon energy of 2.96 eV as a function of the square root of time after excitation for a PFO film spun from cyclopentanone solution (open circles). The solid line represents the best fit to the data assuming a decay based purely on Förster energy transfer to randomly distributed β-phase chromophores (see text).

$$I_D = I_0 \exp\left(-\frac{t}{\tau} - 2\gamma\sqrt{t}\right), \tag{3}$$

where τ is the natural lifetime of the glassy phase in the absence of the acceptor (i.e., the β phase), and γ is related to the Förster radius R_0 via

$$R_0 = \left(\frac{3}{2\sqrt{\pi^3}}\frac{\sqrt{\tau_0}\gamma}{c_\beta}\right)^{1/3} \tag{4}$$

with c_β being the density of β-phase chromophores and τ_0 the radiative lifetime of the glassy phase.[27,28] Here, the Förster radius R_0 corresponds to the separation between donor and acceptor chromophores at which transfer of an excitation from the donor to the acceptor is as likely to occur as *radiative* decay on the donor. The *effective* Förster radius R_0^{eff}, on the other hand, is the donor-acceptor separation at which transfer of an excitation from the donor to the acceptor is as likely to occur as *any other means of donor de-excitation*. The two radii are linked through

$$R_0^{\text{eff}} = \phi^{1/6} R_0, \tag{5}$$

where Φ is the quantum efficiency of the donor.[28]

Typical natural lifetimes measured for the glassy phase of PFO are of the order of a few hundred picoseconds.[9,29] Since the transfer from the glassy phase to the β phase occurs on a much faster time scale, the first part of the exponential in Eq. (3) may be neglected. Plotting the PL decay of the glassy phase at 2.96 eV on a semilogarithmic scale against the square root of time after excitation should consequently lead to a linear appearance of the data, which is what we observe (see Fig. 6). The description of the excitation transfer in terms of a Förster model therefore seems appropriate here.

Figure 6 shows the best fit to these data using Eq. (3) (and neglecting the natural donor decay) from which we obtain a value of $\gamma = 0.305 \pm 0.009\ \mathrm{ps}^{-1/2}$. In order to extract the Förster radius R_0 from this value using Eq. (4), the radiative lifetime of the glassy phase τ_0 and the chromophore density of the β phase c_β need to be known. Ariu *et al.*[9] have determined the PL quantum efficiencies at room temperature for an as-spun-cast glassy and a β-phase containing film to be $\Phi = 0.53$ and 0.55, respectively, with a corresponding natural PL lifetime of $\tau = 430 \pm 10$ ps for both films. Assuming a relation of $\tau = \Phi \tau_0$ between the natural and the radiative lifetimes,[30] we arrive at a value of $\tau_0 = 811 \pm 19$ ps for the glassy phase. To obtain an estimate of the chromophore density of the β phase, c_β, we link this parameter to the chromophore density of the as-spun-cast glassy phase c_g using

$$c_\beta = f b c_g, \tag{6}$$

where f is the fraction of the total chromophores present in the β phase and b is a factor which accounts for changes to the chromophore density due to conformational changes between the glassy and the β phase. Stevens *et al.* have determined a ground state density $c_g = 2 \times 10^{19}\ \mathrm{cm}^{-3}$ for PFO in a purely glassy phase from careful modeling of photobleaching experiments.[31] In order to determine f we consider that the radiative lifetime of the glassy phase and the β phase appear to be very similar indicating an almost identical oscillator strength for both phases. The fraction of β-phase chromophores in the film we investigated should therefore be the same as the β-phase contribution to the absorption, that is, $f = 0.25$. To address the way in which conformational changes between the glassy and the β phase affect the average chromophore density in a film containing some β-phase chains we need to take into account that in the β phase the intrachain correlation length was found[6] to be longer (22 nm) than in the glassy phase (8 nm) by a factor of $r = 2.75$. Assuming that a chromophore comprises one correlated chain segment, the numbers n_g and n_β of glassy phase and β-phase chromophores supported on one chain are related to the chain length L through $L = n_g \times 8\ \mathrm{nm} + n_\beta \times 22\ \mathrm{nm}$. In a purely glassy phase film, on the other hand, the whole chain consists of a number n_g' of glassy phase chromophores, or $L = n_g' \times 8$ nm. The reduction in the total number of chromophores due to the presence of some β phase in the film is therefore given by

$$b = \frac{n_g + n_\beta}{n_g'} = \frac{n_g + n_\beta}{n_g + r n_\beta}, \tag{7}$$

and with the fraction $f = n_\beta/(n_g + n_\beta)$ we obtain

$$b = \frac{1}{1 + f(r-1)} \approx 0.70. \tag{8}$$

However, additional influence on the chromophore density from the presence of the β phase may originate from changes in the interchain order. The formation of a β phase has been shown to be correlated with an enhancement of interchain order with respect to the glassy phase.[6] This could result in denser packing of chromophores, corresponding to an increase in b. However, the fast transfer dynamics we observe indicate that the two phases are well intermixed, so that these effects should be relatively small. The parameter b is therefore likely to lie somewhere in the range between 0.7 and 1, or $b = 0.85 \pm 0.15$. Estimating a 10% error in the values of c_g and f, we obtain a β-phase chromophore density of $c_\beta = (0.43 \pm 0.10) \times 10^{19}\ \mathrm{cm}^{-3}$ for our sample, and using Eq. (4) we determine a Förster radius of $R_0 = 8.2 \pm 0.6$ nm for excitation transfer from the glassy to the β phase. It should be noted that the *effective* Förster radius for this transfer may be much smaller, depending on the quantum efficiency of the film [see Eq. (5)]. It would be interesting to compare this value to the Förster radius R_0^g found for excitation transfer occuring solely between chromophores of the glassy phase. Meskers *et al.*[32] have undertaken a detailed study of the exciton migration in poly(2-ethylhexyl fluorene) (PF2/6), which does usually not support the formation of a β phase[2,33] and find an effective Förster radius of 3 nm for a sample which has a natural PL lifetime of 300 ps. If we assume the radiative lifetime of excitons located on glassy chains in PFO and PF2/6 to be similar, the PF2/6 sample studied by Meskers *et al.* should have had a quantum efficiency of 0.37 and consequently a Förster radius $R_0^g \approx 3.5$ nm according to Eq. (5). This Förster radius for transfer within the glassy phase of PF2/6 (3.5 nm) is significantly lower than the Förster radius we determine for exciton transfer from the glassy to the β phase in PFO (8.2 nm). Such a result should be expected since the spectral overlap between the emission and the absorption of the glassy phase is rather limited, while the emission of the glassy phase of PFO overlaps to a large extent with the (0-0) transition in the β-phase absorption.

Finally, some caution is required when applying Förster's theory to these systems, since the exciton in conjugated polymers tends to be partly delocalized over a chain segment and may therefore no longer be considered as a point dipole. Recent quantum chemical calculations have indicated that for chain segments separated by a few angstroms significant deviations from Förster's theory are to be expected.[34] These effects should be strongest at very early times after excitation ($\leqslant 1$ ps) when the transfer dynamics are dominated by nearest-neighbor transfers. It has also been suggested[35,36] that excitation transfer in conjugated polymers is generally preceeded by migration of excitons within the donor. However, for the sample we investigated, the β-phase concentration is so high that direct transfer of excitons to the β phase should be the most dominant transfer mechanism.

IV. CONCLUSIONS

We have presented a detailed study of the interrelationship between morphology and photophysics in thin films of PFO. Small amounts of the crystalline β phase dominate the emission characteristics. The formation of the two phases during spin coating can be controlled reliably through the choice of the boiling point and solubility parameter of the solvent. A Franck-Condon analysis has shown that the planar chains are characterized by a low Huang-Rhys parameter, consistent with well delocalized excited states, while the nonplanar chains of the glassy phase show high values for

the Huang-Rhys parameter. The close intermixing of the two phases and the large spectral overlap of emission from the glassy phase and absorption from the β phase lead to efficient transfer on a subpicosecond time scale with a Förster radius of about 8 nm. As a result, the steady state emission spectra show a significant fraction of emission from the β phase if only a few percent of the chains are planarized.

ACKNOWLEDGMENTS

The authors thank J. S. Kim for suggestions and insightful discussions. We would like to acknowledge the Cambridge Commonwealth Trust (A.L.T.K.), the Royal Society (A.K.), Peterhouse Cambridge (A.K.), and St. John's College Cambridge (L.M.H.) for financial support.

*Author to whom correspondence should be addressed. Email address: ak10007@cam.ac.uk

[1] U. Scherf and E. J. W. List, Adv. Mater. (Weinheim, Ger.) **14**, 477 (2002).
[2] D. Neher, Macromol. Rapid Commun. **22**, 1365 (2001).
[3] M. Grell, W. Knoll, D. Lupo, A. Meisel, T. Miteva, D. Neher, H.-G. Nothofer, U. Scherf, and A. Yasuda, Adv. Mater. (Weinheim, Ger.) **11**, 671 (2001).
[4] T. Miteva, A. Meisel, W. Knoll, H. Nothofer, U. Scherf, D. C. Müller, K. Meerholz, A. Yasuda, and D. Neher, Adv. Mater. (Weinheim, Ger.) **13**, 577 (2001).
[5] K. S. Whitehead, M. Grell, D. D. C. Bradley, M. Jandke, and P. Strohriegl, Appl. Phys. Lett. **76**, 2946 (2000).
[6] M. Grell and D. C. C. Bradley, Adv. Mater. (Weinheim, Ger.) **11**, 895 (1999).
[7] A. J. Cadby, P. A. Lane, H. Mellor, S. J. Martin, M. Grell, C. Giebeler, D. C. C. Bradley, M. Wohlgenannt, C. An, and Z. V. Vardeny, Phys. Rev. B **62**, 15 604 (2000).
[8] E. J. W. List, C.-H. Kim, A. K. Naik, U. Scherf, G. Leising, W. Graupner, and J. Shinar, Phys. Rev. B **64**, 155204 (2001).
[9] M. Ariu, D. G. Lidzey, M. Sims, A. J. Cadby, P. A. Lane, and D. C. C. Bradley, J. Phys.: Condens. Matter **14**, 9975 (2002).
[10] M. Grell, D. C. C. Bradley, X. Long, T. Chamberlain, M. Inbasekaram, E. P. Woo, and M. Soliman, Acta Polym. **49**, 439 (1998).
[11] M. Ariu, D. G. Lidzey, M. Lavrentiev, D. C. C. Bradley, M. Jandke, and P. Strohriegl, Synth. Met. **116**, 217 (2001).
[12] M. Ariu, M. Sims, M. D. Rahn, J. Hill, A. M. Fox, D. G. Lidzey, M. Oda, J. Cabanillas-Gonzalez, and D. D. C. Bradley, Phys. Rev. B **67**, 195333 (2003).
[13] H.-G. Nothofer, Ph.D. Thesis, Universität Potsdam, 2001 (Logos Verlag, Berlin, 2001). ISBN 3-89722-668-52001.
[14] J. Brandrup, E. H. Immergut, and E. A. Grulke, *Polymer Handbook*, 4th edition (Wiley, New York, 1999).
[15] M. Grell, D. D. C. Bradley, G. Ungar, J. Hill, and K. S. Whitehead, Macromolecules **32**, 5810 (1999).
[16] S. Guha, J. D. Rice, Y. T. Yau, C. M. Martin, M. Chandrasekhar, H. R. Chandrasekhar, R. Guentner, P. S. de Freitas, and U. Scherf, Phys. Rev. B **67**, 125204 (2003).
[17] H. Bässler and B. Schweitzer, Acc. Chem. Res. **32**, 173 (1999).
[18] M. Pope and C. E. Swenberg, *Electronic Processes in Organic Crystals and Polymers* (Oxford University Press, New York, 1999).
[19] P. K. H. Ho, J. S. Kim, N. Tessler, and R. H. Friend, J. Chem. Phys. **115**, 2709 (2001).
[20] M. Ariu, D. G. Lidzey, and D. D. C. Bradley, Synth. Met. **111–112**, 607 (2000).
[21] C. Ramsdale and N. C. Greenham, Adv. Mater. (Weinheim, Ger.) **14**, 212 (2002).
[22] S. Tretiak, A. Saxena, R. L. Martin, and A. R. Bishop, Phys. Rev. Lett. **89**, 097402 (2002).
[23] S. Karabunarliev, M. Baumgarten, E. R. Bittner, and K. Müllen, J. Chem. Phys. **113**, 11 372 (2000).
[24] S. Karabunarliev, E. R. Bittner, and M. Baumgarten, J. Chem. Phys. **114**, 5863 (2001).
[25] M. B. Johnston, L. M. Herz, A. L. T. Khan, A. Köhler, A. G. Davies, and E. H. Linfield, Chem. Phys. Lett. **377**, 256 (2003).
[26] T. Förster, Z. Naturforsch. A **4a**, 321 (1949).
[27] L. M. Herz, C. Silva, R. H. Friend, R. T. Phillips, S. Setayesh, S. Becker, D. Marsitsky, and K. Müllen, Phys. Rev. B **64**, 195203 (2001).
[28] R. C. Powell, J. Lumin. **11**, 1 (1975).
[29] L. M. Herz and R. T. Phillips, Phys. Rev. B **61**, 13 691 (2000).
[30] N. C. Greenham, I. D. W. Samuel, G. R. Hayes, R. T. Phillips, Y. A. R. R. Kessener, S. C. Moratti, A. B. Holmes, and R. H. Friend, Chem. Phys. Lett. **241**, 89 (1995).
[31] M. A. Stevens, C. Silva, D. M. Russell, and R. H. Friend, Phys. Rev. B **63**, 165213 (2001).
[32] S. C. J. Meskers, J. Hubner, M. Oestreich, and H. Bassler, J. Phys. Chem. B **105**, 9139 (2001).
[33] G. Leiser, M. Oda, T. Miteva, A. Meisel, H.-G. Nothofer, U. Scherf, and D. Neher, Macromolecules **33**, 4490 (2000).
[34] D. Beljonne, G. Pourtois, C. Silva, E. Hennebicq, L. M. Herz, R. H. Friend, G. D. Scholes, S. Setayesh, K. Müllen, and J. L. Bredas, Proc. Natl. Acad. Sci. U.S.A. **99**, 10982 (2002).
[35] E. J. W. List, C. Creely, G. Leising, N. Schulte, A. D. Schluter, U. Scherf, K. Mullen, and W. Graupner, Chem. Phys. Lett. **325**, 132 (2000).
[36] A. R. Buckley, M. D. Rahn, J. Hill, J. Cananillas-Gonzalez, A. M. Fox, and D. C. C. Bradley, Chem. Phys. Lett. **339**, 331 (2001).